BULLETIN OF THE POLISH ACADEMY OF SCIENCES
TECHNICAL SCIENCES, Vol. 58, No. 4, 2010
DOI: 10.2478/v10175-010-0046-y

Ultrashort pulses supported by SESAM absorber

A. JASIK*, J. MUSZALSKI[1], J. GACA[2], M. WÓJCIK[2], and K. PIERŚCIŃSKI[1]

[1] Institute of Electron Technology, 32/46 Lotników Ave., 02-668 Warszawa, Poland
[2] Institute of Electronic Materials Technology, Wólczyńska St. 133, Warszawa, Poland

Abstract. We have developed a mode-locked diode-pumped Yb:KYW laser generating nearly band-width limited pulses as short as 101 fs. At 1.1 W absorbed power and 3% transmission output coupler, the laser delivers 150 mW for pulse duration of 110 fs, what corresponds to an efficiency of 14%. It was achieved using semiconductor saturable absorber mirror (SESAM) grown by molecular beam epitaxy. SESAM contains a distributed Bragg reflector (DBR) completed by single quantum well (SQW) playing role of an absorbing layer. The absorbers were crystallized in accordance with the predicted structure parameters under optimised growth conditions. The resonant-like type of structures ensured relatively high enhancement factor due to antireflective properties of SiO_2 capping material and a wavelength independence of a group delay dispersion. The optimisation of the growth conditions of both an absorbing layer and DBR structure were widely carried out. Optical reflectance and high resolution X-ray diffraction have been used for characterization and verification of DBR structures. It results in reduction of the nonsaturable absorption in SESAM and self-starting mode-locking of the ultrashort pulses.

Key words: DBR, SESAM, modelocking, femtosecond pulses.

1. Introduction

An efficient passive mode-locking can be realised by insertion of a nonlinear element – a saturating absorber – into the optical path of a laser resonator. For convenience such absorber is most often integrated with a distributed Bragg reflector (DBR) constituting semiconductor saturable absorber mirrors (SESAMs) [1]. SESAMs suited for ultrashort laser pulse generation require absorbing materials with a fast temporal response of the nonlinear absorption and a DBR structure with very high reflectivity. A standard approach to obtain sub-ps response time is to use the epitaxial layers grown at low temperature (LT) under As reach conditions [2]. It results in generation of the As antisite defects located in the mid of the band gap and plying role of carrier traps. It causes the increase of a carrier recombination rate and in consequence a self-started generation of short pulses. Optical reflectivity and properties of DBRs depend on many factors such as: the contrast of refractive indexes between the alternating layers, the number of periods [3], and structure perfection, which means: uniformity of the chemical composition and thickness of the layers, the shape and roughness of the interfaces. To obtain the reflectivity of DBR close to unity the precise control of the growth parameters has to be performed.

In this work we have investigated the influence of the number of periods on the crystal perfection of DBR heterostructures. We have also verified how the substrate rotation rate enhances the spatial uniformity of the DBR. Then the optimized growth conditions of DBR structures were used to obtain complete structure of SESAM. The operation parameters were tested in Z-shaped resonator of Yb:$KY(WO_4)_2$ laser.

2. SESAM structure design

In order to ensure the SESAM ability to generate the sub-ps pulses in self staring mode locking regime, we had to control the main structure parameters of SESAM, which influence the carrier dynamic characteristics: the group delay dispersion (GDD) and the enhancement factor ξ. GDD describes the phase dependency of the reflected wave on the wavelength and it is defined as the second derivative of a phase with respect to the angular frequency. The wavelength independent GDD is required for the generation of short and nearly transform limited pulses. The enhancement factor is understood as the maximum field intensity in the structure relative to the incoming field intensity. A higher enhancement factor results in lower saturation fluence and higher modulation depth.

A SESAM heterostructure consists of a DBR mirror and an absorber layer. Because the absorber has different refractive index than the high index DBR layer and also because of the high index contrast of the semiconductor and air, the absorber itself and the surrounding layers form an optical cavity, which determines the device operation. The absorber layer has been located just beneath the surface in order to shorten additionally the device response time. A proximity of the surface allows for an efficient diffusion of the carriers and fast non-radiative recombination on surface states. The design was calculated using a transfer-matrix formalism. The GaAs and AlAs refractive indexes were calculated after Aframowitz [4]. The dispersion of a complex refractive index of the InGaAs QW absorber was determined using a spectrally resolved elipsometry.

*e-mail: ajasik@gazeta.pl

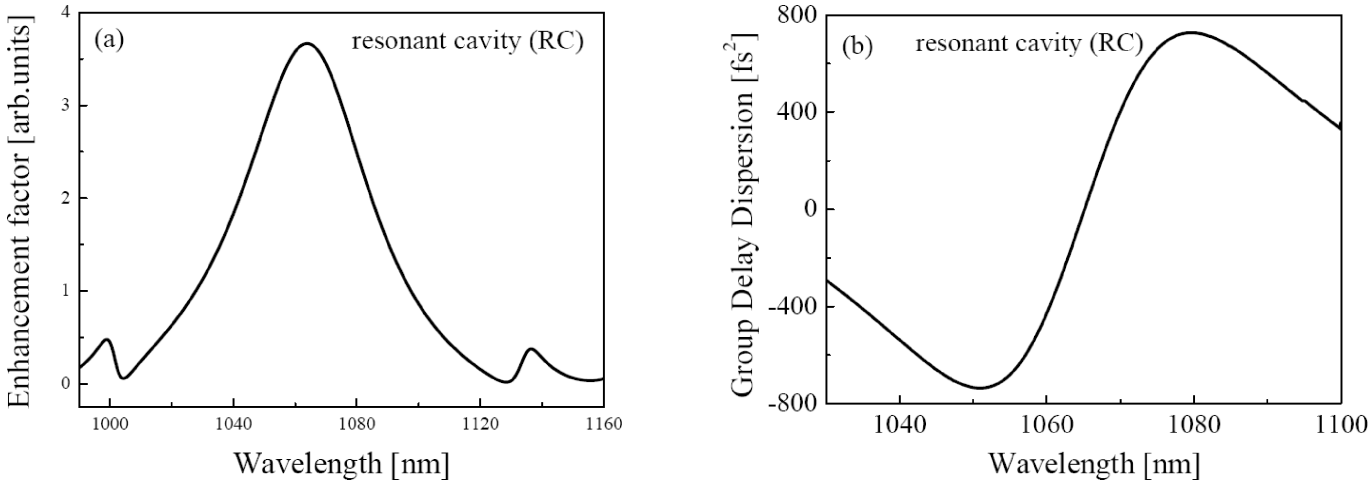

Fig. 1. Calculated enhancement factor ξ (a) and group delay dispersion GDD (b) vs. the operation wavelength for SESAM structures with resonant cavity (RC)

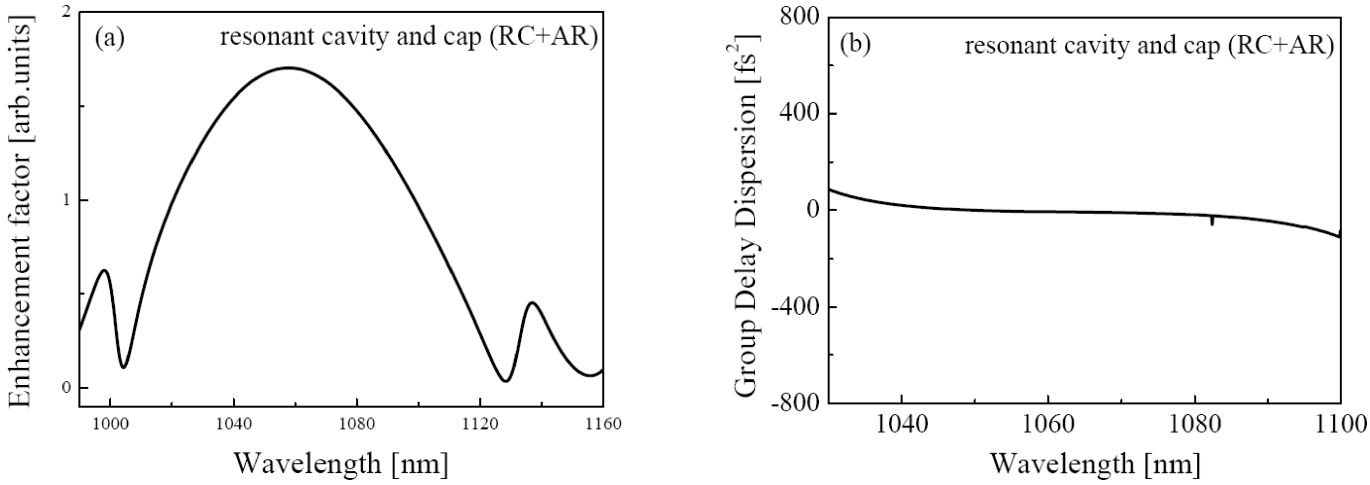

Fig. 2. Calculated enhancement factor ξ (a) and group delay dispersion GDD (b) vs. the operation wavelength for SESAM structures with resonant cavity with SiO_2 anti-reflective cap layer (RC+AR)

When the resonant cavity is applied, an anti-node of the electromagnetic field intensity is placed on the surface, thus at the absorber located just beneath the surface, the enhancement factor is high (Fig. 1a). Nevertheless this design suffers from the GDD wavelength dependence (Fig. 1b).

In order to flatten the GDD we have designed a $\lambda/4n_r$ thick dielectric (SiO_2) layer to be deposited directly on the surface. This happens at the expense of the lower enhancement factor in the consequence of the reflectivity decrease of the semiconductor air interface (Fig. 2a), but such spectral shape of GDD is the most favorable for device operation (Fig. 2b). The whole structure of SESAM is presented in Fig. 3.

In the growth direction the SESAM structure contains a 24-pair AlAs/GaAs distributed Bragg reflector (DBR) but the top quarter-wavelength layer of GaAs is extended by approximately an additional quarter-wavelength layer. The $In_{0.26}GaAs$ absorber layer is placed beneath the surface and capped by 5nm GaAs layer. The structure is completed by the low-refractive index dielectric quarter-wave layer of SiO_2.

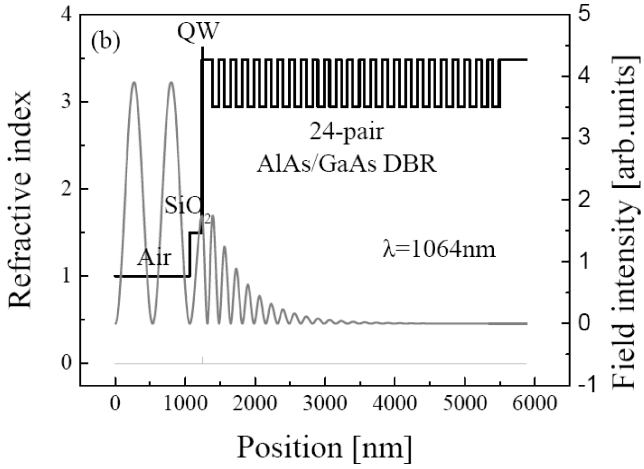

Fig. 3. The refractive-index (black line) and calculated standing wave intensity (gray line) profiles for resonant cavity SESAM with SiO_2 anti-reflective layer (RC+AR)

3. DBR epitaxy

Investigated DBR heterostructures were crystallized by molecular beam epitaxy (MBE). The growth was carried out in three-chamber Riber 32P reactor with Bayard-Alpert gauge for flux measurements and RHEED gun operated at 9 keV. Prior to starting growth the GaAs substrate was heated to 580°C under As_4 beam to remove native oxide. The substrate temperature was measured with both thermocouple and pyrometer. The desorption of the native oxide was confirmed by observation of RHEED pattern changes. Subsequently, the substrate was heated up to 630°C for 5 min to degas residual surface impurities and then cooled down to 580°C to begin the structure crystallization. Both GaAs and AlAs layers were grown with the rate of 2.5 Å/s under As-rich condition and with the (2×4) surface reconstruction. The growth of AlAs/GaAs Bragg reflectors was carried out at the substrate temperature of 530°C. The deposition of the whole heterostructure was performed without any growth interruptions.

All technological processes are listed in Table 1. The samples are divided into four groups, depending on the purpose of their investigations.

Table 1
The growth conditions of AlAs/GaAs DBR structures

set	samples	period number	couple of materials used	rotation rate [min^{-1}]	λ [nm]
1	MBE1	15	AlAs/GaAs	5	1051
	MBE2	15	AlAs/GaAs	5	1054
2	MBE3	**15**	AlAs/GaAs	5	1170
	MBE4	**23**	AlAs/GaAs	5	1120
3	MBE5	15	AlAs/GaAs	**5**	1068
	MBE6	15	AlAs/GaAs	**30**	1065

The first group of samples was grown as a reference set. The same epitaxial conditions were used. The main objective of the crystallization was to prove that the optical reflectance is not sufficiently precise tool to characterize the reflection quality of the mirrors, especially when the reflectivity exceeds 98%, and simultaneously to test the precision and usability of the HR XRD method for this purpose.

The heterostructures of the second group differ by the number of periods. They were grown in order to investigate the interface roughening as a function of the number of periods. The reason for this study may be justified as follows. The reflectivity of DBR consisting of 15 periods, is predicted theoretically to be above 98%. It is sufficient to optimize the resonant wavelength and reflection properties of the mirror. Moreover the value higher then 98% approaches the limits of reflectivity measurement reliability. On the other hand, in SESAM the reflectivity of 99.5% or higher is required, so 23 or more pairs are needed. The prediction of the mirror reflectivity follows from the calculations based on the formula reported by Sale [3]. To calculate the refractive index n for GaAs, AlAs, $Al_{0.3}GaAs$ for specific photon energy, we used formula developed by Kokubo and Ohta [5]. Therefore samples with 15 and 23 periods were grown and investigated. The difference of 8 periods should be sufficient to trigger off the roughening of heterointerfaces.

The third set of heterostructures contains samples grown with different substrate rotation rates. It was expected that increasing rotation rate would improve the thickness uniformity, the growth front flatness and consequently the interface sharpness.

4. Results and discussion of DBR investigation

For all structures the measured peak reflectivity exceeds the value of 99.0% independently on used technological conditions and number of periods. The measured resonant wavelengths are listed in Table 1. The reflectivity spectra of MBE1 and MBE2 samples were found to be very similar in the overall shape as well as in peak reflectivity (Fig. 4). On the basis of these results, the precise determination of the highest mirror reflectivity is not possible. Therefore we employed HR XRD technique to find DBR samples with the best structural quality. In Fig. 5, (004) diffraction curves for the MBE1 and MBE2 samples, recorded by high-resolution X-ray diffractometer using CuK_α radiation are presented.

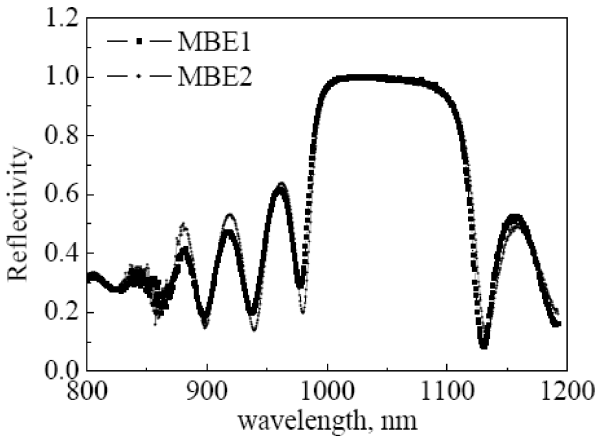

Fig. 4. The reflectivity spectra of MBE1 and MBE2 samples

For MBE1 sample no broadening of the substrate and satellite peaks is observed, all peaks are symmetrical. This suggests, that there is neither bending of the layer stack nor disturbance of periodicity in the sample, as opposed to the MBE2 sample, where asymmetrical satellite peaks can be seen, which may indicate some kind of structure deformation. To explain the nature of observed deformation, the theoretical diffraction curves were calculated employing a software based on Darwin dynamical diffraction theory. The calculated diffraction curves that proved to be the best fit to experimental data are also presented in Fig. 5. The analysis showed that for the MBE1 DBR the best fit between experimental and calculated diffraction curves was achieved assuming that the whole structure is lattice matched and each out of 15 periods is the same. In the case of MBE2 DBR sample the best fit between experimental and theoretical curves was achieved under the assumption that at the beginning of the deposition process the periodicity was lost and then recovered after the deposition of few periods.

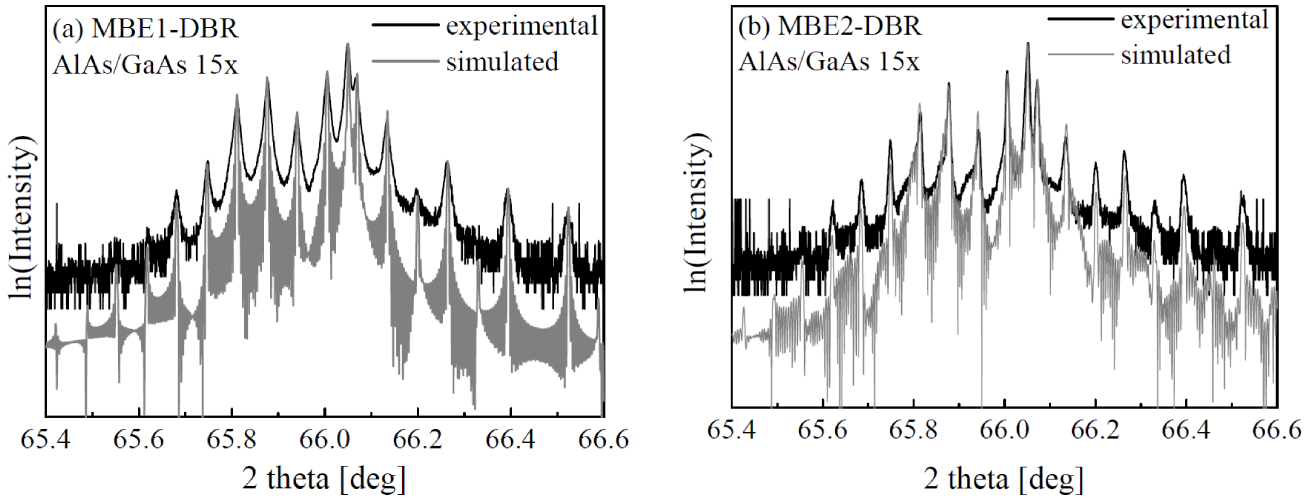

Fig. 5. Experimental and calculated (004) diffraction curves for MB1 (a) and MBE2 (b) DBR structures

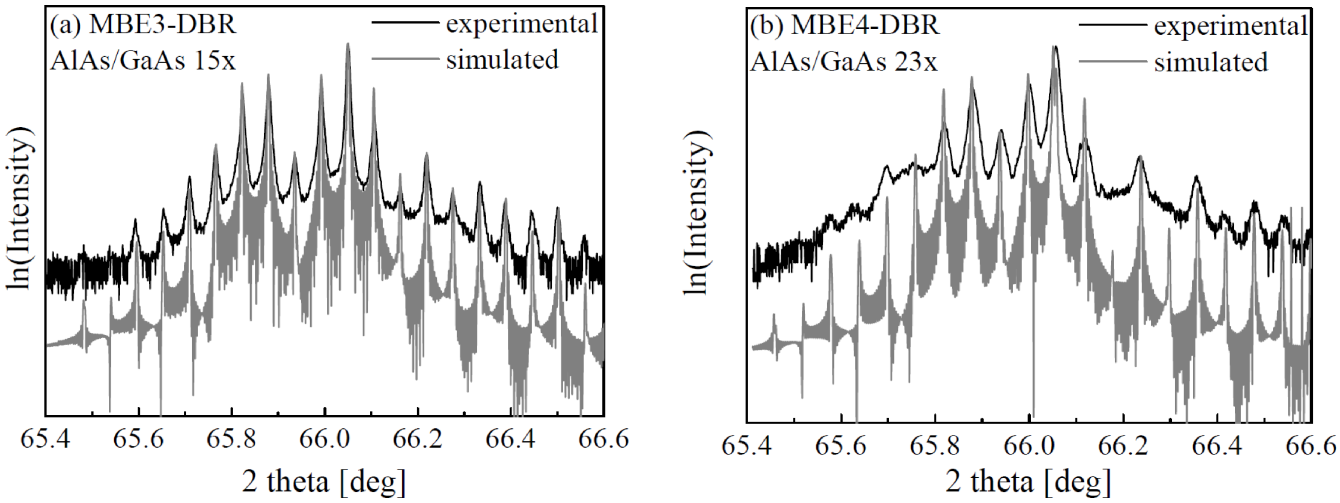

Fig. 6. Experimental and calculated (004) diffraction curves for MBE3 (a) and MBE4 (b) DBR structures

It is obvious that the reflectivity for DBRs with grater number of periods is higher than that measured for DBRs with lower number of periods. On the other hand, enhanced roughening of growth front due to higher number of interfaces decreases the reflectivity. Therefore the influence of the period number on the DBR reflectivity can not be estimated via the simple comparison of the reflectivity value for two DBR structures. The investigation of the crystal perfection for DBR structures with different number of periods solves this problem. In Fig. 6 the simulated and experimental X-ray diffraction curves of MBE3 and MBE4 samples are plotted.

The samples differ only by the number of periods as shown in Table 1. The key epitaxial conditions were the same for both structures. Although these DBR structures have different number of periods, it seems there are no differences between their peak reflectivity. As can be seen in Fig. 6, the satellite peaks are more broadened for the 23-period MBE4 sample, but the broadening is practically independent of the order of the satellite reflection. These results indicate that generally the MBE4 sample is of poorer crystal quality as compared to that of MBE3 one, its interface roughness is greater, but the deviation from periodicity in both samples is relatively small.

The sharpness of the interfaces and the spatial uniformity of the layer thickness can be increased by improving the flatness of the growth front. Under the fixed epitaxial conditions; kinetic and thermodynamic, the two-dimensional growth can be enhanced by the assuring a uniform transport of the particles and its uniform incorporation into the growing crystal. Both are the function of the substrate rotation rate [6]. The typical value of the rotation rate used in MBE processes was 5 turns per 1 minute. The rotation rate applied during the MBE6 epi-growth was 6 times higher then the typical one and was equal to 30 turns per 1 minute. The reflectivity spectra measured at several points along the radius of MBE5 and MBE6 structures are shown in Fig. 7.

Differences in spectral position of the stop-bands between adjacent measurements for compared samples are the same. It means that the lateral homogeneity of the structure does not depend on the rotation rate of the substrate. The con-

figuration of the holder/manipulator and the effusion cells in the growth chamber enforces and redefines the growth rate at each point of the substrate. Nevertheless the increase of the crystal perfection in the growth direction was observed by HR XRD measurements (Fig. 8). The diffraction data for MBE6 sample are characterized by better pronounced and narrower satellite peaks then its counterpart for MBE5 sample. That means that the crystal perfection of the samples improves with the increase of the substrate rotation rate during the growth process. This dependence can be explained by more uniform substrate temperature distribution of faster rotating wafer; thus more uniform spaces mobility on the growing crystal surface and uniform incorporation probability.

It is known, that the defects favors the liberation of the energy cumulated in the strained material. At low defect density at the interfaces the strain energy is maintained, the misfit dislocation generation is suppressed and the lattice remains strained. This was observed by X-ray topography measurements. The transmission topograms in crystallographically equivalent reflections of 220 for both MBE5 and MBE6 DBRs are presented in Fig. 9.

As it is shown in Fig. 9a, the relaxation process by formation of MDs is clearly observed for DBR5 grown at the slow rotation rate. The MDs are distributed in two orthogonal direction <110> and <1–10> in plane of (001) (only one is shown). The MDs are homogenously distributed and their density is equal in both crystallographic directions. In case of DBR6, where no relaxation process is observed, no MDs are visible. This confirms the results obtained by HR XRD measurements. The DBR6 structure is fully strained. Previous results reported by Mazuelas et al. show [7], that fully strained undoped AlAs/GaAs DBR designed for an operation wavelength of 980 nm was grown only up to 10 periods (total thickness of 1.5 μm). In our case it is 15 period DBR6 structure for 1060 nm with total thickness of 2.5 μm.

In this stage of investigation, the growth conditions of DBR structures with close to unity reflectivity are optimized. The precise control of the low temperature epitaxial growth of $In_{0.26}GaAs$ layer playing role of absorbing material allows us to performed SESAM heterostructure [8]. The complete devices was obtained when the SiO_2 layer was deposited by plasma enhanced chemical vapor deposition.

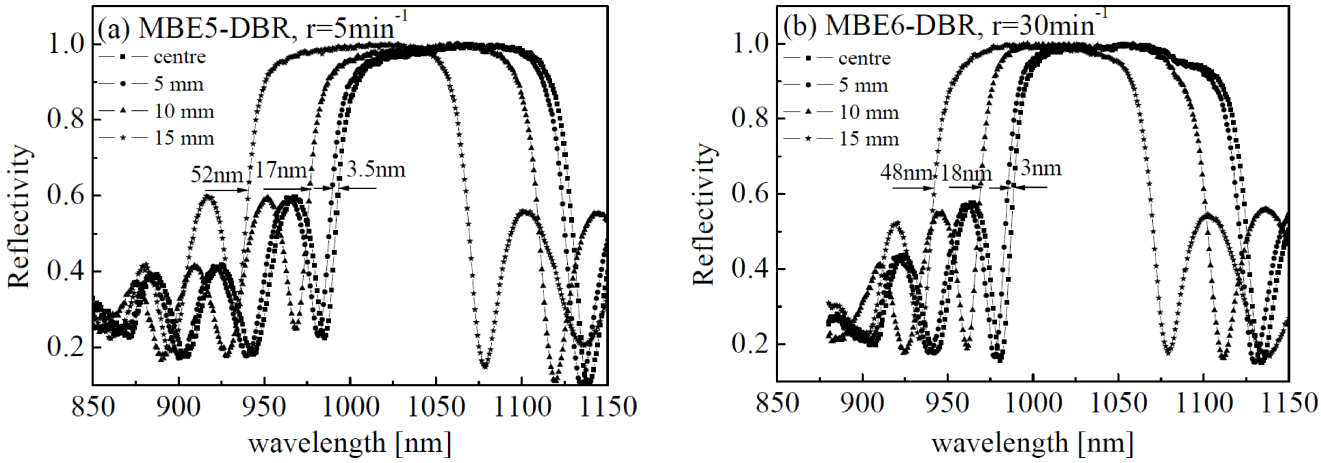

Fig. 7. Reflectivity spectra of 15 pair AlAs/GaAs Bragg reflectors grown at standard rotation of 5 run/min (a) and higher rotation of 30 run/min b)

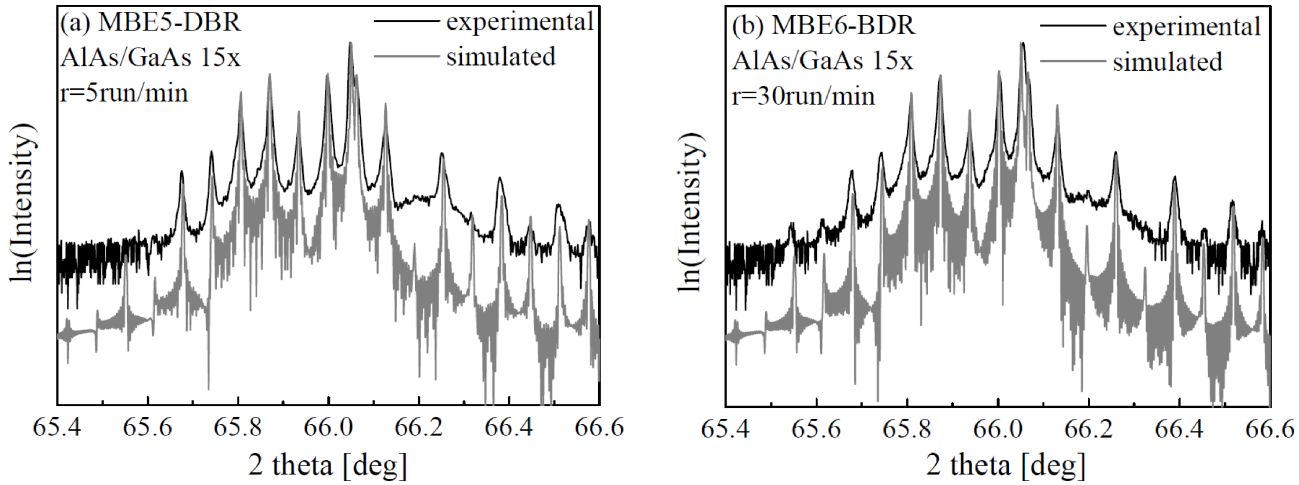

Fig. 8. Experimental and calculated (004) diffraction curves for MBE5 (a) and MBE6 (b) DBR structures

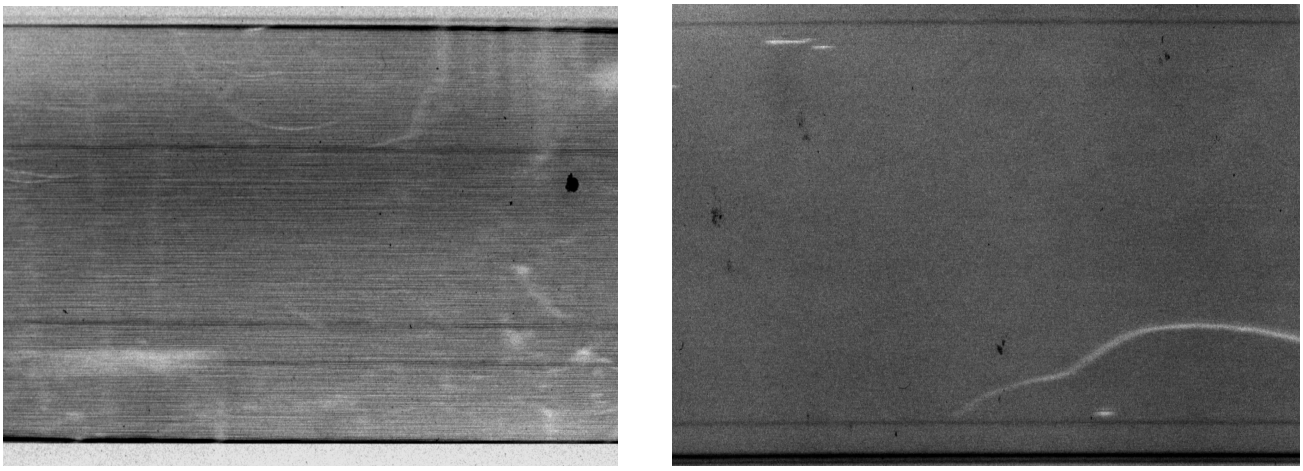

Fig. 9. Lang transmission topograms in the equivalent crystallographic reflections of 220 performed with X-ray radiation of MoKαs obtained for DBRs: MBE5 (left) and MBE6 (right) samples

5. SESAM operation

Mode-locked operation was tested for the heterostructures of SESAM in the common z-shaped astigmatically compensated cavity. The scheme of optical set up is presented in Fig. 10.

The arm of the output coupler contained two SF10 prisms with a tip-to-tip distance of 39 cm. Focussing on the SESAM1 was realized by an $f = -150$ mm spherical mirror. The experiment was performed with Yb-doped potassium yttrium tungstate Yb:KY$(WO_4)_2$ (Yb:KYW) as a gain medium. This material has very promising properties for constructing efficient femtosecond oscillators: large emission and absorption cross section, broad emission bandwidth and good thermal conductivities [9, 10]. The KYW crystal was pumped at 980 nm by a broad stripe laser diode. The emission bandwidth was about 3.5 nm.

The passive mode-locking of the pumped Yb:KYW crystal was achieved. Using a 3% transmission output coupler the pulses as short as 110 fs were achieved. The Fig. 11 shows the intensity autocorrelation trace and fit assuming a sech^2 pulse shape.

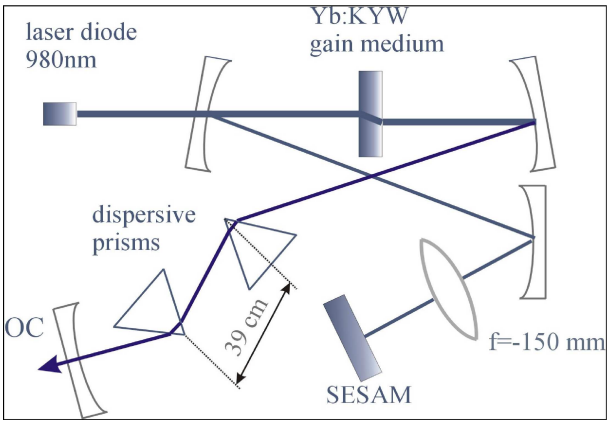

Fig. 10. The scheme of a z-shaped Yb:KY$(WO_4)_2$ laser cavity

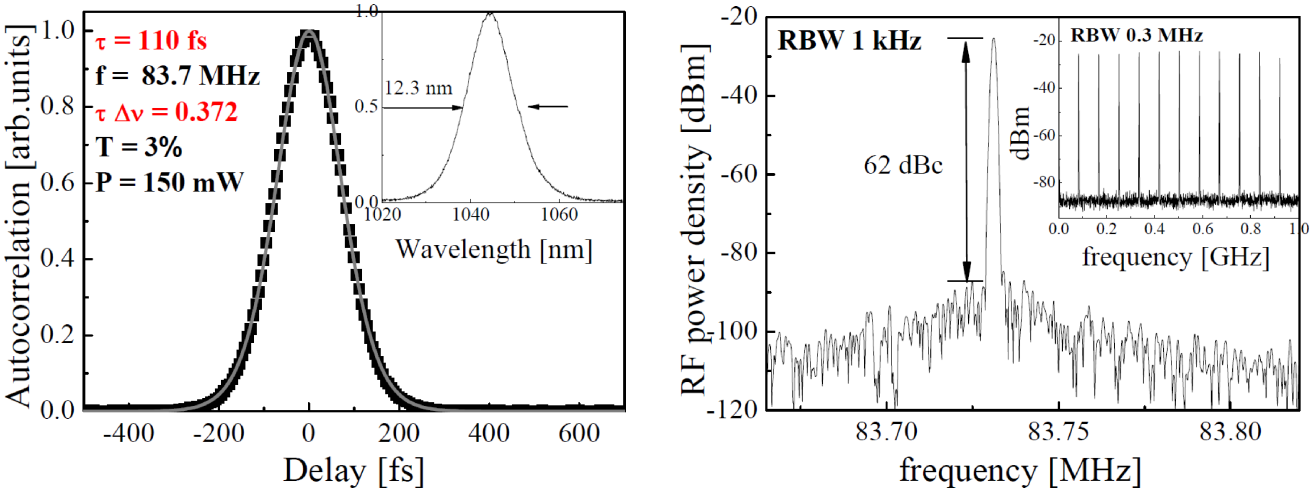

Fig. 11. Intensity autocorrelation and optical spectrum (inset) (left) and radio frequency spectrum (right) of the mode-locked Yb:KYW gain medium with SESAM

The corresponding optical spectrum is centred at 1049 nm and has a FWHM of 12.3 nm. This results in the time-bandwidth product of 0.372. We recorded the radio frequency spectrum, indicating 62 dBc extinction ratio of the fundamental beat note at 83.7 MHz without spurious modulations, as measured with 1 kHz resolution bandwidth (Fig. 11). The average output power amounts to 150 mW and the repetition rate to 83.7 MHz, resulting in a energy per pulse of 1.8 nJ. This corresponds to the peak power of 14.5 kW. The incident pump power was 1.1 W, which resulted in a conversion efficiency as high as 14%. A conversion efficiency comparable to the results of Klopp et al. [11] was achieved but at a longer pulse duration of 134 fs. Similar results were received by Paunescu et al. [12] using a Yb:KGW /(Yb:KYW) crystal with pulse durations of 100 fs/(106 fs) and output power of 126 mW/(92 mW) but applying a transmission output coupler of 2% and an input power of 1.57 W. The conversion efficiency is 8%/(6%) although the introduced losses in the absorber structure were less than 0.3%.

Using an 1% output coupler the shortest pulses of 101 fs at 16 mW output power were obtained. In the recorded frequency spectrum, no spurious modulations are visible down to 70 dBc, which indicates a stable CW mode locking. The time-bandwidth product of 0.358 is slightly above the theoretical value of 0.315 for a sech^2 pulse shape.

6. Conclusions

We have demonstrated the stable self-starting passive CW mode locking of the Yb:KYW laser at about 1046 nm using pseudomorphic InGaAs SESAM device. The SESAM was based on the resonant-like cavity obtained between DBR and the air-semiconductor interface. The DBR structures were designed for maximum reflectivity. Since it is a challenge to measure the reflectivity values above 99%, the HR XRD has been applied to solve this problem by the detailed characterization of the DBR crystal quality. The influence of the number of periods and the rotation rate of substrate on the abruptness of interfaces and the crystal perfection and hence on the reflection performance of DBRs has been investigated. It has been found, by means of X-ray investigation, that the defect density and the surface roughness is higher for heterostructures with higher number of interfaces. The rotation rate of the substrate influences the performance homogeneity of the DBR structures. The increase of homogeneity in the growth direction was observed for structures grown at the higher rotation rate of substrate. The optimized growth parameters of DBR were adopted for SESAM crystallization. The mode-locked operation of SESAM was tested in the z-shaped cavity. At 1.1 W input power the average output power was 150 mW for the generated pulses as short as 110 fs.

Acknowledgements. The authors would like to thank Uwe Griebner and Andreas Schmidt, at Max Born Institute for the autocorrelation measurements, and also Krzysztof Hejduk from the Institute of Electron Technology for SiO_2 growth processes using PECVD.

This work was partially supported by Polish Committee of Scientific Research Grant PBZ MiN-009/T11/2003.

REFERENCES

[1] U. Keller, D.A.B. Miller, G.D. Boyd, T.H. Chiu, J.F. Ferguson, and M.T. Asom, "Solid-state low-loss intracavity saturable absorber for Nd:YLF lasers: an antiresonant semiconductor Fabry-Perot saturable absorber", *Opt. Lett.* 17, 505–507 (1992).

[2] D.C. Look, "Molecular beam epitaxial GaAs grown at low temperature", *Thin Solid Films* 231, 61–73 (1993).

[3] T.E. Sale, *Vertical Cavity Surface Emitting Lasers*, Research Studies Press Ltd., Somerset, 1995.

[4] M.A. Aframowitz, "Refractive Index of $Ga_{1-x}Al_xAs$", Solid State Commun. 15, 59–63 (1974).

[5] Y. Kokubo and I. Ohta, "Refractive index as a function of the photon energy for AlGaAs between 1.2eV and 1.8eV", *J. Appl. Phys.* 81 (4), 2042–2045 (1997).

[6] G.B. Stringfellow, *Organometallic Vapour Phase Epitaxy: Theory and Practice*, Academic Press, Utah, 1989.

[7] A. Mazuelas, R. Hey, M. Wassermeier, and H.T. Grahn, "Strain compensation in highly carbon doped GaAs/AlAs distributed Bragg reflectors", *J. Cryst. Growth* 383, 175–176 (1997).

[8] A. Jasik, J. Muszalski, J. Gaca, M. Wójcik, M. Kosmala, and K. Piersciński, "SESAM – nonlinear semiconductor absorber – characterization and technology of production", *3rd Nanotechnology Conf.* 1, CD-ROM (2009), (in Polish).

[9] N.V. Kuleshov, A.A. Lagatsky, A.V. Podlipensky, V.P. Mikhailov, and G. Hubert, "Pulsed laser operation of Y b-dope d $KY(WO_4)_2$ and $KGd(WO_4)_2$", *Opt. Lett.* 22, 1317–1319 (1997).

[10] G. Métrat, M. Boudeulle, N. Muhlstein, A. Brenier, and G. Boulon, "Nucleation, morphology and spectroscopic properties of Yb^{3+}-doped $KY(WO_4)_2$ crystals grown by the top nucleated floating crystal method", *J. Cryst. Growth* 197, 883–888 (1999).

[11] P. Klopp, V. Petrov, U. Griebner, and G. Erbert, "Passively mode-locked Yb-KYW laser pumped by a tapered diode laser", *Optics Express* 10 (2), 108–111 (2002).

[12] G. Paunescu, J. Hein, and R. Sauerbrey, "100-fs diode-pumped Yb:KGW mode-locked laser", *Appl. Phys.* B 79, 555–557 (2004).